Octave Bandwidth High-Performance Microstrip-to-Double-Ridge-Waveguide Transition

José R. Montejo-Garai, Laila Marzall, *Graduate Student Member, IEEE*, and Zoya Popović, *Fellow, IEEE*

***Abstract*— This letter presents a microstrip-to-double-ridge-waveguide transition with high performance in the octave bandwidth operation between 6 and 12 GHz. The structure is based on a three-chamfered-step transformer supported directly over the microstrip line without soldering. The electric contact is ensured by the pressure between the first step of the transformer and a groove in the microstrip line. The transition is formed by two halves, minimizing the manufacturing complexity and the loss contact. A sequential procedure has been followed in the design process. Initially, a port directly feeding the planar structure has been considered, obtaining a simulated return loss level better than 25 dB in the whole operation band. Afterward, feeding through an SubMiniature version A (SMA) coaxial connector, a simulated return loss level better than 20 dB has been obtained. In order to verify the above theoretical simulations, a back-to-back arrangement has been measured, connecting two similar transitions. The prototype shows an insertion loss for a single transition lower than 0.8 dB in the 67% fractional bandwidth from 6 to 12 GHz.**

***Index Terms*— Dual-ridge waveguide, microstrip, octave band, transition.**

I. Introduction

ACTIVE phased arrays [1] or high throughput satellite (HTS) [2] T/R modules demand high-performance components, easy integration, and wide operation bandwidth. In these systems, low-loss and well-matched transitions between different guided-wave components play a crucial role.

Planar structures, such as microstrip lines, are common in microwave systems because of their compact size, low cost, and integration capability with active components including a monolithic microwave-integrated circuit (MMIC). On the other hand, waveguides are suitable when power handling and low loss are required. In addition to the above, if a wide monomode bandwidth is required, a double-ridge waveguide [3] is often used. Consequently, a transition between both transmission media is needed in order to gain the best of both technologies.

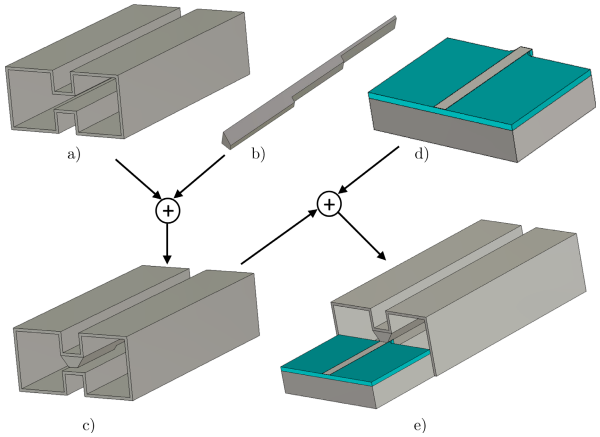

Fig. 1. Schematic of the microstrip-to-double-ridge waveguide transition. The elements are (a) empty double-ridge waveguide, (b) chamfered three-step transformer, (c) double-ridge waveguide with the transformer, (d) microstrip line with added groove for support and suitable contact, and (e) complete structure.

The main specifications for the transition between the quasi-TEM mode of the microstrip and the TE mode of the double-ridge rectangular waveguide are low insertion loss, suitable matching, reduced size, and manufacturing repeatability.

Microstrip-to-rectangular waveguide transitions were extensively analyzed, mainly the inline configuration [4]–[7]. Different structures have been developed in order to improve the wideband response. A contactless transition working in a 28% fractional bandwidth is presented in [8]. Using a ridge structure on the high-permittivity thin-film material, a 37% is demonstrated in [9]. An extension to a 53% fractional bandwidth by means of a dielectric tip and a tapered double-ridged waveguide section is shown in [10].

However, the direct transition between the microstrip and the double-ridge waveguide is not specifically addressed in the technical literature, to the best of our knowledge. An approximate design is presented in [11]. Here, we attempt to fill this gap, showing a high-performance structure with straightforward assembly and operating over an octave bandwidth or 67% fractional bandwidth (Fig. 1). The experimental results confirm that the new transition is well suited for the wide-bandwidth operation, in particular for feeding a phase array from 6 to 12 GHz.

Manuscript received March 6, 2020; revised April 13, 2020 and May 6, 2020; accepted June 3, 2020. Date of publication June 23, 2020; date of current version July 7, 2020. This work was supported in part by the Office of Naval Research under Award N00014-19-1-2487. The work of José R. Montejo-Garai was supported by the Spanish Government programs, (ADDMATE) TEC2016-76070-C3-2-R (AEI/FEDER/UE) and Fulbright-MICINN FMECD-ST-2019. The work of Laila Marzall was supported in part by the Coordenacao Aperfeicoamento de Ensino Superior (CAPES), Brazil. *(Corresponding author: José R. Montejo-Garai.)*

José R. Montejo-Garai is with the Grupo de Electromagnetismo Aplicado, Information Processing and Telecommunications Center, Universidad Politécnica de Madrid, 28040 Madrid, Spain (e-mail: joseramon.montejo@upm.es).

Laila Marzall and Zoya Popović are with the Department of Electrical, Computer and Energy Engineering, University of Colorado, Boulder, CO 80309 USA (e-mail: laila.marzall@colorado.edu; zoya.popovic@colorado.edu).

Color versions of one or more of the figures in this letter are available online at http://ieeexplore.ieee.org.

Digital Object Identifier 10.1109/LMWC.2020.3000283

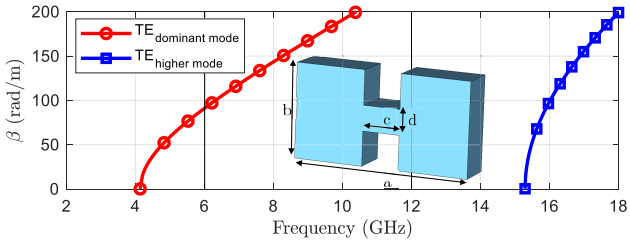

Fig. 2. Dispersion diagram of the double-ridge waveguide, showing the propagation constants for the TE-dominant mode and the TE higher mode, with $a = 21.27$ mm, $b = 9.9$ mm, $c = 4.47$ mm, and $d = 3.63$ mm.

II. Design Process of the Proposed Transition

The modular scheme of the transition between the microstrip line and the double-ridge waveguide is shown in Fig. 1. The empty waveguide [Fig. 1(a)] is modified by adding a chamfered three-step transformer [Fig. 1(b)], as shown in Fig. 1(c). A groove in the microstrip [Fig. 1(d)] is the support for the pressure contact with the transformer. The complete transition is shown in Fig. 1(e).

Starting from the empty waveguide [Fig. 1(a)], the first task is to determine its dimensions for operation in the octave band from 6 to 12 GHz. The four parameters, *a, b, c*, and *d*, shown in Fig. 2, are optimized to obtain the required monomode bandwidth. The cutoff frequency for the fundamental mode is 4.13 GHz and for the next higher mode is 15.29 GHz, where both modes are TE. The substrate chosen for the design is Rogers TMM3 with permittivity $\epsilon_r = 3.27$ and thickness 0.762 mm.

The key matching element in the transition is a chamfered transformer, where the first step has the same width as the microstrip line, i.e., 1.72 mm for 50 Ω [Fig. 1(d)]. This profile [Fig. 1(b)] confines the electromagnetic field in a very efficient way and in a short distance from the microstrip line to the volume between the two ridges, and is easy to manufacture since it has only one discontinuity between the steps. The number of steps, three in this design, and their lengths and heights are optimized using an algorithm based on the simulated annealing method [12], [13] to fulfill the theoretical matching level (25 dB). The geometrical dimensions are shown in Fig. 3(c).

A groove in the microstrip [Fig. 1(d)] is included as support for the pressure contact without soldering. It contributes also to efficient matching, working like a taper between the quasi-TEM mode of the microstrip line and the TE mode in the waveguide.

Fig. 3(a) shows the transition, directly feeding the planar circuit (port included in the figure), with open boundary conditions. The size of the microstrip port in the simulation is important: the port needs to be large enough to enclose a significant part of the fundamental quasi-TEM mode, while being sufficiently small to avoid higher order waveguide modes [14]. Fig. 4 shows that the obtained return loss is higher than 25 dB in the entire operation band.

The relative radiated power calculated from power conservation ($1.0–|s_{11}|^2–|s_{21}|^2$) considering ideal elements (perfect conductors and loss-less dielectric) is lower than the 10%.

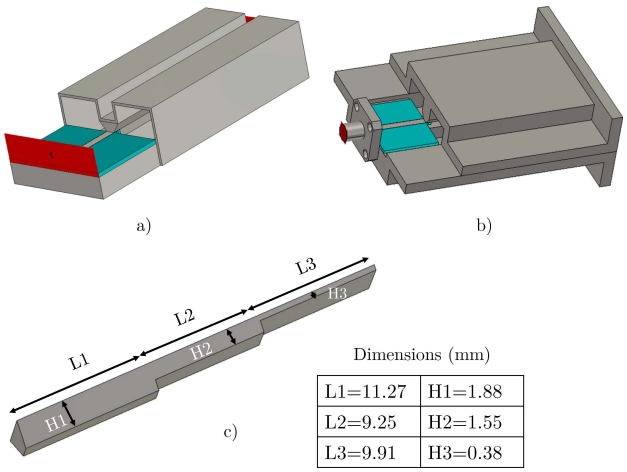

Fig. 3. (a) Microstrip line to double-ridge waveguide transition, feeding directly the planar structure (port included). (b) Microstrip line to double-ridge waveguide transition including the SMA connector and feeding with a coaxial port. (c) Geometrical dimensions of the three-step transformer.

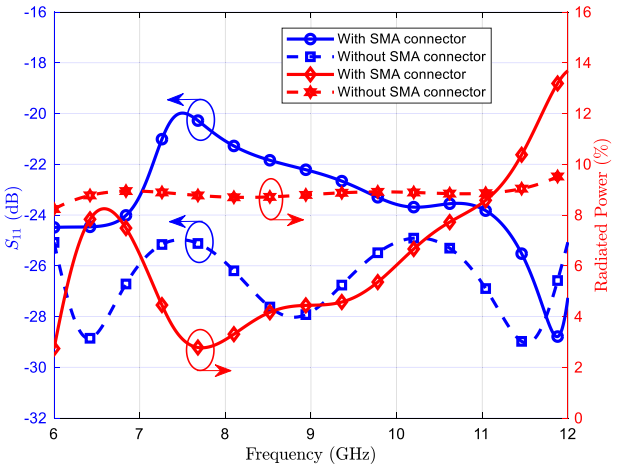

Fig. 4. Simulated responses of the microstrip-line-to-double-ridge-waveguide transition with perfect conductors and lossless dielectric, considering open boundary conditions. (a) Feeding directly the planar structure [Fig. 3(a)]: return loss on the left and percentage of radiated power on the right. (b) Including the SMA connector and feeding with coaxial port [Fig. 3(b)]: return loss on the left and percentage of radiated power on the right.

This loss is not usually specified in the technical literature but is not negligible. Due to the wide bandwidth, enclosing the microstrip between the metallic walls generates spurious resonant modes and the open boundary condition is necessary.

Next, a more realistic study is performed including the SubMiniature version A (SMA) connector and the coaxial feed [Fig. 3(b)]. In this way, the uncertainty regarding the size of the microstrip port is eliminated and the device is very close to that manufactured. Fig. 4 shows the simulated response. The introduction of the SMA connector reduces the return loss from 25 to 20 dB around 7.5 GHz. However, the radiated power has decreased notably, except in the upper band beyond 11 GHz.

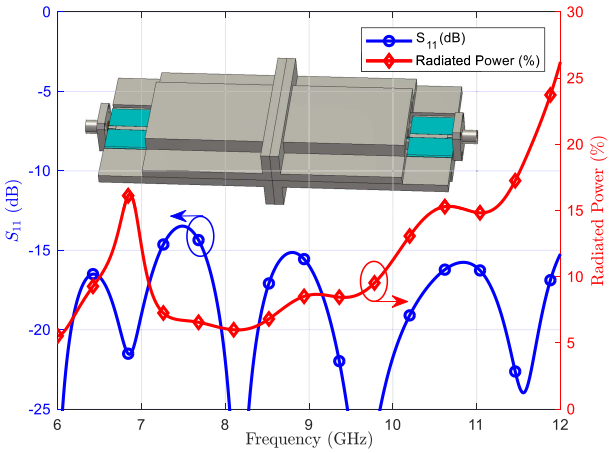

Fig. 5. Simulated response of the microstrip-line-to-double-ridge-waveguide transition including the SMA connector and feeding with coaxial ports in a back-to-back configuration: return loss on the left and percentage of radiated power on the right. Perfect conductors and lossless dielectric are assumed.

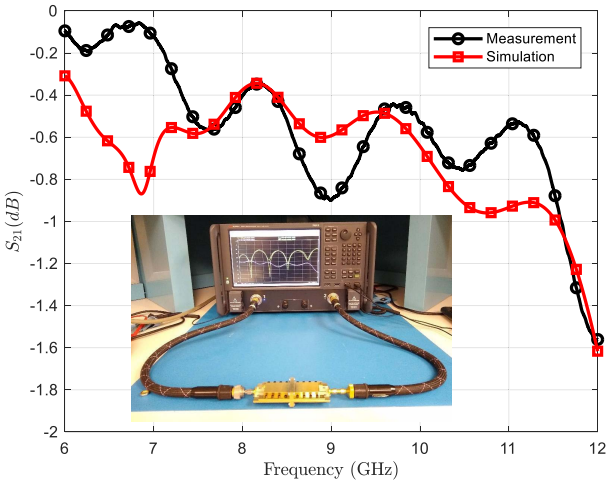

Fig. 6. Comparison of the insertion loss between the full-wave simulation of the transition in a back-to-back configuration and the measurement considering the conductivity of brass $\sigma_{\text{brass}} = 15.9$ MS/m, copper $\sigma_{\text{Cu}} = 58.9$ MS/m, and the dielectric loss ($\tan\delta = 0.002$). Inset: photograph of prototype in the test setup.

Finally, Fig. 5 shows the simulated response of the above structure in a back-to-back configuration, for direct comparison to measurement. The radiated power is, as expected, two times that of the single transition.

III. Experimental Results

In order to verify the theoretical results, two equal transitions are manufactured in brass, and the return and insertion loss is measured in a back-to-back configuration. The inset in Fig. 6 shows the experimental characterization with a Keysight N5241B vector network analyzer, and the photograph in the inset in Fig. 7 shows the connection of both transitions.

Fig. 6 shows the comparison between the simulated insertion loss and the measurement considering the conductivity of brass $\sigma_{\text{brass}} = 15.9$ MS/m, copper $\sigma_{\text{Cu}} = 58.9$ MS/m, and dielectric loss ($\tan\delta = 0.002$). The agreement is good, and at some frequency points, the measured match is better than the simulation because of radiation. The highest value of the insertion loss of a single transition is below 0.8 dB.

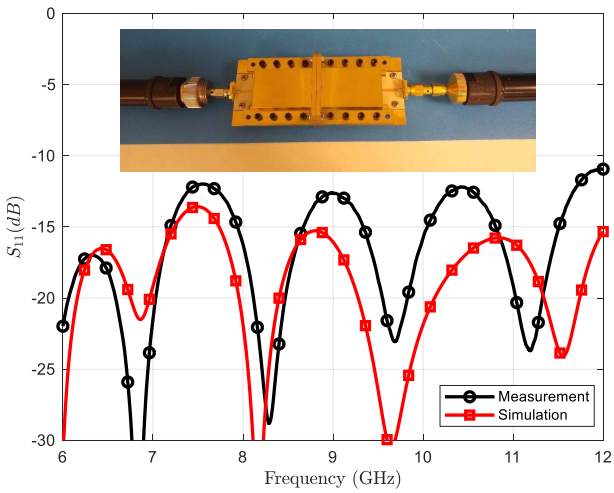

Fig. 7. Comparison of the return loss between the full-wave simulation of the transition in a back-to-back configuration and the measurement considering the conductivity of brass $\sigma_{\text{brass}} = 15.9$ MS/m, copper $\sigma_{\text{Cu}} = 58.9$ MS/m, and the dielectric loss ($\tan\delta = 0.002$). Inset: photograph of the prototype in back-to-back configuration.

TABLE I

State-of-the-Art: Microstrip-to-Double-Ridge-Waveguide Transition

Work	Frequency Band (GHz and %)	Length (mm and λ_o [1])	Insertion) Loss (dB)	Return Loss (dB) [2]	Structure
[7]	8.5-9.5 (11%)	77.93 ($2.34\lambda_o$)	1.1	> 10	Rectangular waveguide
[8]	72-95 (28%)	3.62 ($1.0\lambda_o$)	0.8	> 10	Ridge waveguide
[9]	60-87.5 (37%)	5.5 ($1.35\lambda_o$)	1.35	> 10	Dielectric ridge
[10]	55-95 (53 %)	45.72 ($11.43\lambda_o$)	1.8	> 10	Dielectric tip
This Work	**6-12 (67%)**	**30.43 ($0.91\lambda_o$)**	**0.8**	$> \mathbf{11}$	**Double-ridge waveguide**

[1] Free space wavelength computed at the center frequency of the design band; [2] Back-to-back configuration.

Fig. 7 shows the comparison between the simulated return loss and the measurement considering, as previously, the lossy materials. The agreement is reasonable, considering that the measured response falls within the limits of a sensitivity analysis when the milling accuracy of ± 0.05 μm, the dispersion of the permittivity $\epsilon_r = 3.27$ of ± 0.032, and the alignment process are considered.

IV. Conclusion

A novel octave bandwidth (6–12 GHz) microstrip-line-to-double-ridge waveguide transition is designed, manufactured, and measured. A simple structure, composed of two parts without soldering, results in high-performance operation and easy assembly. Two analyses are shown: initially, feeding the microstrip line directly (theoretical ideal port), and, later, feeding with an SMA coaxial connector. The simulated and measured results in a back-to-back configuration are in good agreement. The insertion loss of a single transition is lower than 0.8 dB over the 67% relative bandwidth. A summary of the comparison with other works is shown in Table I, where the properties of the presented design are highlighted.

REFERENCES

[1] J. L. Salazar, R. H. Medina, and E. Loew, "T/R modules for active phased array radars," in *Proc. IEEE Radar Conf. (RadarCon)*, Arlington, VA, USA, May 2015, pp. 1125–1133.

[2] Y. Guan, F. Geng, and J. H. Saleh, "Review of high throughput satellites: Market disruptions, affordability-throughput map, and the cost per bit/second decision tree," *IEEE Aerosp. Electron. Syst. Mag.*, vol. 34, no. 5, pp. 64–80, May 2019.

[3] S. Hopfer, "The design of ridged waveguides," *IEEE Trans. Microw. Theory Techn.*, vol. 3, no. 5, pp. 20–29, Oct. 1955.

[4] T. Araki and M. Hirayama, "A 20-GHz integrated balanced mixer," *IEEE Trans. Microw. Theory Techn.*, vol. 19, no. 7, pp. 638–643, Jul. 1971.

[5] G. E. Ponchak and R. N. Simons, "A new rectangular waveguide to coplanar waveguide transition," in *Proc. IEEE Int. Dig. Microw. Symp.*, Dallas, TX, USA, vol. 1, May 1990, pp. 491–492.

[6] H.-W. Yao, A. Abdelmonem, J.-F. Liang, and K. A. Zaki, "Analysis and design of microstrip-to-waveguide transitions," *IEEE Trans. Microw. Theory Techn.*, vol. 42, no. 12, pp. 2371–2380, Dec. 1994.

[7] Y. Zhang, J. A. Ruiz-Cruz, K. A. Zaki, and A. J. Piloto, "A waveguide to microstrip inline transition with very simple modular assembly," *IEEE Microw. Wireless Compon. Lett.*, vol. 20, no. 9, pp. 480–482, Sep. 2010.

[8] A. Aljarosha, A. U. Zaman, and R. Maaskant, "A wideband contactless and bondwire-free MMIC to waveguide transition," *IEEE Microw. Wireless Compon. Lett.*, vol. 27, no. 5, pp. 437–439, May 2017.

[9] C. Hannachi, T. Djerafi, and S. O. Tatu, "Broadband *E*-band WR12 to microstrip line transition using a ridge structure on high-permittivity thin-film material," *IEEE Microw. Wireless Compon. Lett.*, vol. 28, no. 7, pp. 552–554, Jul. 2018.

[10] F. Voineau, A. Ghiotto, E. Kerherve, M. Sie, and B. Martineau, "Broadband 55–95 GHz microstrip to waveguide transition based on a dielectric tip and a tapered double-ridged waveguide section," in *IEEE MTT-S Int. Microw. Symp. Dig.*, Honololu, HI, USA, Jun. 2017, pp. 723–726.

[11] Y. Zhou, H.-X. Liu, E. Li, G.-F. Guo, and T. Yang, "Design of a wideband transition from double-ridge waveguide to microstrip line," in *Proc. Int. Conf. Microw. Millim. Wave Technol.*, Chengdu, China, May 2010, pp. 737–740.

[12] R. H. J. M. Otten and L. P. P. P. van Ginneken, *The Annealing Algorithm*. Norwell, MA, USA: Kluwer, 1989.

[13] H. W. Press, A. S. Teukolsky, T. W. Vetterling, and P. B. Flannery, *Numerical Recipes in Fortran 77: The Art of Scientific Computing*, vol. 1, 2nd ed. Cambridge, U.K.: Cambridge Univ. Press, 1986, Ch. 10.

[14] (Jan. 2020). CST-Computer Simulation Technology. [Online]. Available: https://www.cst.com/